AAPT PHYSICS EDUCATION | AMERICAN JOURNAL of PHYSICS

Tunneling through a truncated harmonic oscillator potential barrier

Jeff D. Chalk

Citation: American Journal of Physics **58**, 147 (1990); doi: 10.1119/1.16223
View online: http://dx.doi.org/10.1119/1.16223
View Table of Contents: http://scitation.aip.org/content/aapt/journal/ajp/58/2?ver=pdfcov
Published by the American Association of Physics Teachers

Magnetic Resonance (Harper & Row, New York, 1967).
[9]A. Abragam, *Principles of Nuclear Magnetism* (Oxford U. P., Oxford, 1961).
[10]Newport type 03, Newport Instruments Ltd., Blakelands North, Milton Keynes MK1 45AW, England.
[11]J. M. S. Hutchinson, W. A. Edelstein, and G. Johnson, "A whole-body NMR imaging machine," J. Phys. E **13**, 947–955 (1980).
[12]F. N. H. Robinson, A sensitive nuclear quadrupole resonance spectrometer for 2–60 MHz," J. Phys. E **15**, 814–823 (1982).
[13]Martin Packard and Russel Varian, "Free nuclear induction in the Earth's magnetic field," Phys. Rev. **93**, 941 (1954).
[14]G. S. Waters, "A measurement of the Earth's magnetic field by nulcear induction," Nature **176**, 691 (1955).
[15]G. S. Waters and P. D. Francis, "A nuclear magnetometer," J. Sci. Instrum. **35**, 88 (1958).
[16]P. T. Callaghan and M. Le Gros, "Nuclear spins in the Earth's magnetic field," Am. J. Phys. **50**, 709–713 (1982).
[17]E. L. Hahn, "Nuclear induction due to free Larmor precession," Phys. Rev. **77**, 297–298 (1950).
[18]H. Y. Carr and E. M. Purcell, "Effects of diffusion on free precession in nuclear magnetic resonance experiments," Phys. Rev. **94**, 630–638 (1954).

Tunneling through a truncated harmonic oscillator potential barrier

Jeff D. Chalk
Physics Department, Southern Methodist University, Dallas, Texas 75275

(Received 20 April 1988; accepted for publication 18 March 1989)

The sum of a one-dimensional, truncated harmonic oscillator potential and square well of the same range, defined in the positive half-space, serves as a convenient and instructive example for which the Schrödinger equation may have both bound-state and continuum solutions. A superposition of these solutions is used in a study of barrier penetration by a wave packet representing a particle with an initial position in the region of the potential well. The presence or absence of a bound state in the superposition is shown to be the key factor determining the evolution of the wave packet. If no bound state exists, the probability of the particle having a position within the potential well is a monotonically decreasing function of time. If the superposition includes a bound state, however, this probability oscillates slightly because of an interference between the bound-state and continuum components of the wavefunction.

I. INTRODUCTION

A potential function of rectangular shape is a natural choice for an introduction to the tunneling phenomenon because of the mathematical simplicity provided. The rectangular barrier and square well have been used in discussions of the propagation of a wave packet through a potential.[1–4] In such a discussion, a sequence of "snapshots" of the probability density $|\psi|^2$ provides a very satisfying qualitative view of the evolution of the packet during the tunneling process.

Although the truncated harmonic oscillator potential involves familiar and simple power-series solutions of the Schrödinger equation, it seems that this potential function is overlooked as a useful potential for a pedagogical study of tunneling.[5,6] A sum of truncated harmonic oscillator potential and square well of the same range was used in this article to study the barrier penetration of a wave packet representing a particle with an initial position in the region of the potential well. The investigation was prompted by the author's desire to present to a class in quantum mechanics an interesting alternative to a rectangular potential and an example that emphasizes the continuum solutions.

The potential function considered restricts the motion of a particle of mass m to the half-space $x \geqslant 0$:

$$V(x) = \begin{cases} \infty, & x < 0, \\ -V_0 + \frac{1}{2} m\omega^2 x^2, & 0 < x < a, \\ 0, & x > a. \end{cases} \tag{1}$$

Here, V_0 is the maximum potential depth, a is the range, and ω is the angular frequency. The initial task will be to find bound-state and continuum solutions of the Schrödinger equation. A significant convenience of this potential is the fact that the solutions for the region within the well and in the region of the barrier are one and the same, and can be written down immediately, since they involve the same power series encountered in deriving the solutions for the linear harmonic oscillator. The series is not truncated in this case, however, so that the solutions do not involve Hermite polynomials.

Two sets of potential parameters are considered so as to allow either one or no bound states. Analysis of an assumed initial wavefunction in terms of the two complete sets of energy eigenfunctions will reveal a pronounced difference in the structure of the packets, and the evolution of the packets will differ accordingly. Particular attention is given to the varying probability of the particle having a position within the potential barrier. The results for the two potentials, presented graphically, provide the basis for the final discussion.

II. ENERGY EIGENFUNCTIONS

In order to solve the Schrödinger equation with the potential function of Eq. (1), it is convenient to introduce the parameters $\alpha = (m\omega/\hbar)^{1/2}$, $\zeta = \alpha a$, and $\gamma_0 = V_0/\hbar\omega$, along with the dimensionless variable $\xi = \alpha x$. Also, the number n is suitably defined by the relation

$$E + V_0 = (n + \tfrac{1}{2})\hbar\omega . \tag{2}$$

Accordingly, the Schrödinger equation for the interior region may be written as

$$\frac{d^2\psi}{d\xi^2} + (2n + 1 - \xi^2)\psi = 0, \quad 0 < \xi < \zeta , \tag{3}$$

which will be recognized as the same equation encountered in treating the linear harmonic oscillator. If allowance is made for the boundary condition $\psi(0) = 0$, one then writes down odd solutions of the familiar form[7]

$$\psi_n = A v_n(\xi) e^{-\xi^2/2}, \quad 0 < \xi < \zeta , \tag{4}$$

where $v_n(\xi)$ denotes the series

$$v_n(\xi) = \xi - [2(n-1)/3!]\xi^3 + [2^2(n-1)(n-3)/5!]\xi^5 \pm \cdots , \tag{5}$$

and A denotes a normalization constant. Equation (4) applies both to positive and negative energies. Using the fact that there is no physical solution for $E < -V_0$, one infers from Eq. (2) the inequality $-\frac{1}{2} < n < \gamma_0 - \frac{1}{2}$ for negative energies and $n > \gamma_0 - \frac{1}{2}$ for positive energies.

Now, in the linear oscillator problem the condition that ψ be well behaved as ξ becomes large leads to the restriction of n to integer values, and Eq. (5) is used to introduce odd Hermite polynomials. The potential here is truncated at $\xi = \zeta$, however, so there is no such boundary condition to restrict n, and the series represented by (5) must be regarded as infinite. The number of terms that must be included in a numerical evaluation of v_n will depend on the magnitude of ξ as well as the precision demanded.

In the exterior region, the potential vanishes and the Schrödinger equation may be written as

$$\frac{d^2\psi}{d\xi^2} - (2\gamma_0 - 2n - 1)\psi = 0, \quad \xi > \zeta . \tag{6}$$

Looking first at the bound-state problem, one writes solutions of (6) in the form $\psi_n = F\exp[-(\kappa/\alpha)\xi]$, where $\kappa/\alpha = (2\gamma_0 - 2n - 1)^{1/2}$, and F is a constant. From the requirement that ψ_n and $d\psi_n/d\xi$ be continuous at $\xi = \zeta$, one obtains two equations for A and F, which will be compatible only for certain energies. One thus finds that the allowed values of n are the roots of the transcendental equation

$$v_n'(\zeta) + (\kappa/\alpha - \zeta)v_n(\zeta) = 0 . \tag{7}$$

One must also impose the normalization condition

$$\int_0^\infty |\psi_n|^2 dx = 1 .$$

Then, using the continuity of ψ at $\xi = \zeta$ to express F in terms of A, one derives

$$|A| = \alpha^{1/2}\left(\int_0^\zeta v_n^2 e^{-\xi^2} d\xi + \frac{v_n(\zeta)^2 e^{-\zeta^2}}{2(\kappa/\alpha)}\right)^{-1/2} .$$

The integral appearing in this expression for $|A|$ must, of course, be computed numerically.

It was found that specification of the potential depth and range parameters γ_0 and ζ is sufficient for a determination of $a^{1/2}\psi_n(x)$, and, for the purpose of graphing, the parameter a was set equal to unity. With ω regarded as fixed, two sets were selected, namely,

(1) $\gamma_0 = 1.75$, $\zeta = 5^{1/2}$,

(2) $\gamma_0 = 1.25$, $\zeta = 2$.

For the first set, Eq. (7) allows only one bound state, and for this state n has the value $n_1 = 0.944\,77$ (including here only five significant figures). In the calculation of $v_n(\zeta)$ for n in the neighborhood of n_1, it was found that 29 terms were sufficient to represent this series, and hence determine n_1, to an accuracy of 13 significant figures.

In the case of positive energies, the plane-wave solutions of Eq. (6) are characterized by the wavenumber $k = \alpha(2n + 1 - 2\gamma_0)^{1/2}$, and one may write $\psi_n = B\exp(ik\xi/\alpha) + C\exp(-ik\xi/\alpha)$, where B and C are constants. The continuity conditions at $\xi = \zeta$ may be used to derive the ratio

$$B/C = -e^{-2ika}(w/w^*) ,$$

where

$$w = v_n'(\zeta) - (\zeta - ik/\alpha)v_n(\zeta) .$$

It is convenient at this point to write $w = |w|e^{i(ka+\delta)}$, thereby introducing the phase shift δ.[8] One may then derive

$$\psi_n = -C(e^{i(kx+2\delta)} - e^{-ikx}), \quad x > a .$$

The choice $C = -Ne^{-i\delta}/2i$, where $N = (2m/\pi^2\hbar^2 E)^{1/4}$, provides the so-called energy normalization.[9] That is, the continuum solutions,

$$\psi_E(x) = \begin{cases} \dfrac{N\sin(ka+\delta)v_n(\alpha x)\exp(-\alpha^2x^2/2)}{v_n(\zeta)\exp(-\zeta^2/2)}, & 0 < x < a , \\ N\sin(kx+\delta), & x > a , \end{cases} \tag{8}$$

satisfy the relation

$$\int_0^\infty \psi_{E'}(x)\psi_E(x)dx = \delta(E' - E) . \tag{9}$$

The reader should bear in mind the relation between E and n given by Eq. (2) in ascertaining the dependence of ψ_E on the energy. The series v_n, k, and δ are all naturally regarded as functions of n and are conveniently computed as such, but they are also functions of E in view of this relation.

III. EVOLUTION OF A WAVE PACKET

With the energy eigenfunctions determined, the stage is now set to study the barrier penetration of a wave packet. The assumed initial wavefunction, chosen so as to represent a particle with a very small probability of its position being outside the potential well, is simply expressed as

$$\psi(x,0) = C'xe^{-1.8\alpha x} , \tag{10}$$

where $C' = 2(1.8\alpha)^{3/2}$ in order that the function be properly normalized. A graph of this function is shown in Fig. 1 superimposed on graphs of the potential function and bound-state wavefunction.

The construction and propagation of wave packets is well discussed in textbook literature.[10] For the case that one bound state exists, the wavefunction for $t \geqslant 0$ is written as the superposition

$$\psi(x,t) = C_{n_1}\psi_{n_1}(x)e^{-iE_{n_1}t/\hbar} + \int_0^\infty C(E)\psi_E(x)e^{-iEt/\hbar}\,dE\,, \tag{11}$$

where the coefficients C_{n_1} and $C(E)$ are determined from an analysis of the initial wavefunction in terms of the bound-state and continuum energy eigenfunctions:

$$C_{n_1} = \int_0^\infty \psi_{n_1}(x)\psi(x,0)dx$$

and

$$C(E) = \int_0^\infty \psi_E(x)\psi(x,0)dx\,.$$

After some elementary integration, one finds

$$C_{n_1} = \frac{C'A}{\alpha^2}\int_0^\xi v_{n_1}(\xi)\xi e^{-1.8\xi-\xi^2/2}\,d\xi + C'Fa^2\frac{(\sigma+1)e^{-\sigma}}{\sigma^2}, \tag{12}$$

$$C(E) = \frac{G\sin(ka+\delta)}{v_n(\zeta)\exp(-\zeta^2/2)}\int_0^\xi v_n(\xi)\xi \times\exp\left(-\frac{1.8\xi-\xi^2/2}{2}\right)d\xi + \frac{G\xi e^{-1.8\xi}}{(1.8)^2+(ka)^2} \times\left[\left(1.8\xi+\frac{(1.8)^2-(k/\alpha)^2}{(1.8)^2+(k/\alpha)^2}\right)\sin(ka+\delta) + \left(ka+\frac{2(1.8)(k/\alpha)}{(1.8)^2+(k/\alpha)^2}\right)\cos(ka+\delta)\right], \tag{13}$$

where $\sigma = (1.8+\kappa/\alpha)\xi$ and $G = C'N/\alpha^2$. Use may be made of the series (5) for v_n in numerically computing the integrals appearing in (12) and (13). The final result obtained for the bound-state coefficient in the case of the first potential function is $C_{n_1} = 0.911\,82$, thus showing that the bound state contributes in a major way to the superposition. Equation (13) applies to both sets of potential parameters, and the computer results for $C(E)$ in the two cases reveal a pronounced difference in these functions, as shown in Fig. 2. It should be pointed out that the reversal in sign of $C(E)$ is due to the change in presence of a bound-state component and is not the result of a change in normalization sign of the functions ψ_E. For both potentials the function $C(E)$ rapidly decreases in magnitude and approaches zero as E becomes large.

After the coefficients C_{n_1} and $C(E)$ are obtained, it is very comforting to verify the relation

$$|C_{n_1}|^2 + \int_0^\infty |C(E)|^2\,dE = 1\,,$$

thereby confirming the completeness of the set of eigenfunctions used in constructing the wave packet. The closeness of the check depends, of course, on the accuracy with which the integral is approximated by a discrete sum. For the case in which there exists one bound state, the sum of coefficients squared was found equal to 0.999 98. For the other case, this sum was computed to be 0.999 86.

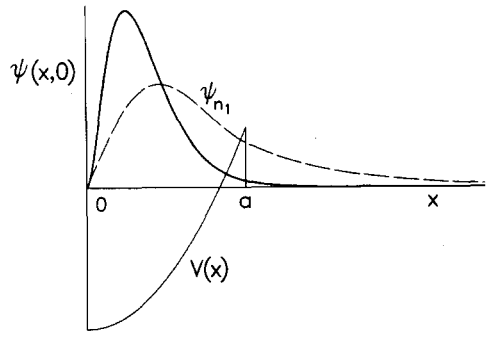

Fig. 1. Initial wavefunction. The graph of the assumed initial wavefunction is superimposed on graphs of the potential function and bound-state wavefunction. This function is expressed as $\psi(x,0) = 2(1.8\alpha)^{3/2}xe^{-1.8\alpha x}$. The potential function $V(x)$ is the sum of a square well of depth V_0 and a truncated oscillator potential $\frac{1}{2}m\omega^2x^2$, both of range a. The parameter V_0 is equal to $1.75\hbar\omega$ and $\alpha^2a^2 = m\omega a^2/\hbar = 5$. For $x<a$, the bound-state wavefunction ψ_{n_1} is proportional to $v_{n_1}(\alpha x)e^{-\alpha^2x^2/2}$, where $v_{n_1}(\alpha x)$ denotes the same power series encountered in the linear oscillator problem, but characterized by the number $n_1 = 0.944\,77$. For $x>a$, ψ_{n_1} is of the form $e^{-\kappa x}$, where $\kappa = \alpha(2.5-2n_1)^{1/2}$.

The final computation of $\psi(x,t)$ for a number of different times employs Eq. (11) and makes use of the results obtained earlier for C_{n_1} and $C(E)$. The numerical integration here is burdensome since the upper limit is infinite. The integral converges fairly rapidly, however, because of the smallness of $C(E)$ for large n, and, in fact, good results (accurate to three significant figures or better) are obtained if the integral is truncated at about $n = 120$.

The evolution of the initial wavefunction was thus determined for the two potential functions considered. Graphs of the probability density $|\psi(x,t)|^2$ for the two cases are shown in Figs. 3 and 4 for four different times. These graphs should be viewed in conjunction with those of Fig. 5 where the probability of the particle having a position within the barrier,

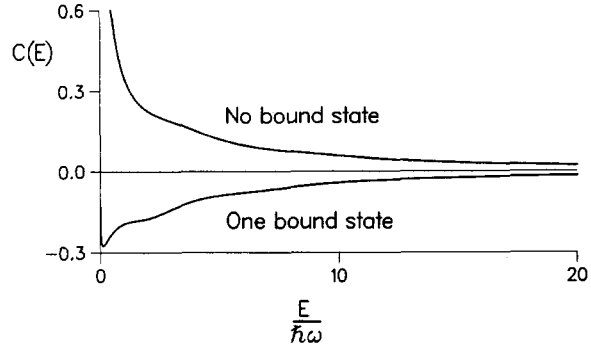

Fig. 2. Continuum coefficients. The initial wavefunction of Fig. 1 is analyzed in terms of the energy eigenfunctions, thereby yielding continuum coefficient functions of the energy. The coefficient function, denoted $C(E)$, is positive for all energies if no bound state exists, and is negative for all energies if there is one bound state.

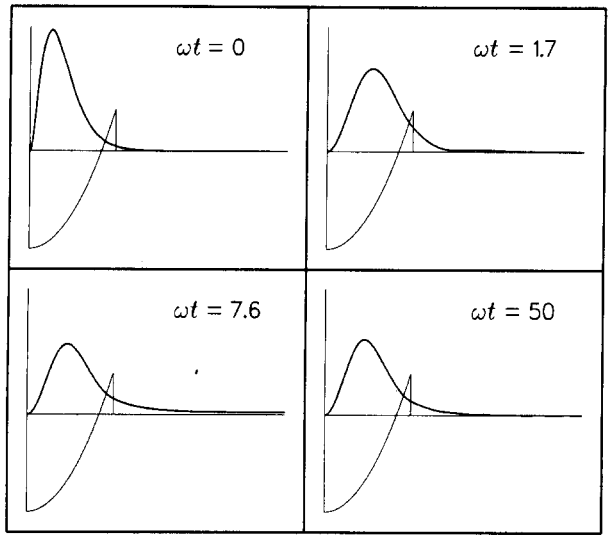

Fig. 3. Evolution of the wave packet of Fig. 1 for the case in which there exists one bound state. The graph of the probability density $|\psi(x,t)|^2$ is superimposed on the graph of the corresponding potential function and is shown at four different times.

$$P_a(t) = \int_0^a |\psi(x,t)|^2\, dx\,, \tag{14}$$

is plotted as a function of t.

IV. DISCUSSION

The graphs of Fig. 3 represent the propagation of the wave packet in the case where there is a bound state, which in fact dominates the superposition. It is observed that the shape of the packet changes rapidly at first as an increasing portion of the probability appears outside the barrier. The peak of the distribution moves to the right initially and then rebounds slightly to the left, where it remains stationary. After a long time has passed ($\omega t = 50$, say), the positive-energy components have tunneled through the barrier and only the bound-state component remains in the neighborhood of the barrier. The decrease in the probability $P_a(t)$ is not monotonic, however. Figure 5 shows that this function passes through two minima, thus underscoring the oscillatory behavior of the packet during the tunneling process.

The graphs of Fig. 4 depict the tunneling in the case where only positive-energy eigenfunctions contribute to the superposition. The height of the probability distribution steadily decreases as an increasingly large percentage of the probability is removed from the vicinity of the barrier. Not really discernible from the graph is a reversal in the direction of motion of the peak at $\omega t = 1.5$ and again at $\omega t = 2.8$. Nevertheless, the function $P_a(t)$ monotonically decreases with time in this case, as shown in Fig. 5.

The behavior of the probability $P_a(t)$ can be understood if one substitutes in the integrand of (14) the expression for $\psi(x,t)$ given by (11). One finds that the expression for $P_a(t)$ reduces to a sum of three terms:

$$\begin{aligned} P_a(t) = {} & C_{n_1}^2 \int_0^a \psi_{n_1}(x)^2\, dx + \int_0^a dx \int_0^\infty C(E)\psi_E(x)\, dE \\ & \times \int_0^\infty C(E')\psi_{E'}(x)\cos\left(\frac{(E-E')t}{\hbar}\right) dE' \\ & + 2C_{n_1} \int_0^a \psi_{n_1}(x)\, dx \int_0^\infty C(E)\psi_E(x) \\ & \times \cos\left(\frac{(E-E_1)t}{\hbar}\right) dE\,. \end{aligned} \tag{15}$$

The second term will monotonically decrease with the passage of time since the factor $\cos[(E-E')t/\hbar]$ oscillates more rapidly as t increases. The third term in (15) will also tend to decrease because of the factor $\cos[(E-E_1)t/\hbar]$, but this same factor provides a modulation of the magnitude so that the decrease is not monotonic. Of course, the first and third terms are not present if there is no bound state.

In summary, the combination of square well and trun-

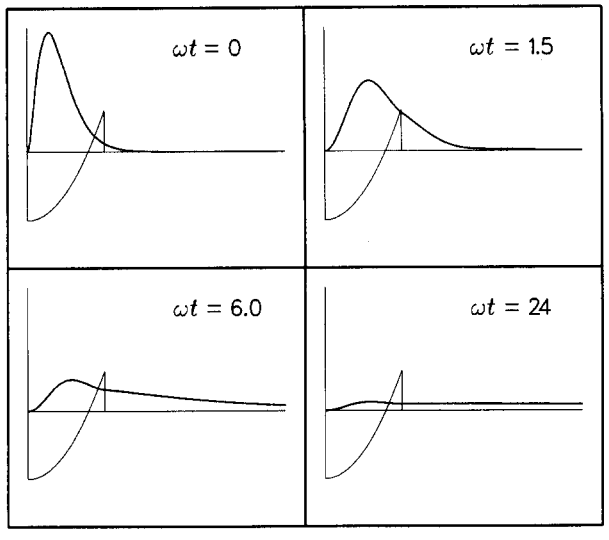

Fig. 4. Evolution of the wave packet of Fig. 1 for the case in which there is no bound state. The graph of the probability density $|\psi(x,t)|^2$ is superimposed on the graph of the corresponding potential function and is shown at four different times.

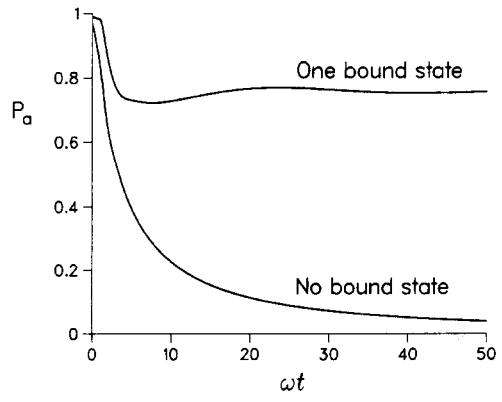

Fig. 5. Probability of the particle having a position within the barrier for the cases in which there exists either one bound state or no bound state. The probability is expressed as $P_a(t) = \int_0^a |\psi(x,t)|^2\, dx$, where a is the range of the corresponding potential function.

cated harmonic oscillator potential of the same range provides a convenient and instructive example of a quantum mechanical system for which exact bound-state and positive-energy solutions may be obtained in closed form. In a pedagogical study of tunneling, the model provides a graphical example of the way in which the positive-energy components of a wave packet "leak" through the barrier, leaving the bound-state component behind. Finally, an interference between the bound and continuum states is shown to underlie oscillatory variations in the probability of the particle being found inside the potential barrier.

[1]Abraham Goldberg, Harry M. Schey, and Judah L. Schwartz, "Computer-generated motion pictures of one-dimensional quantum-mechanical transmission and reflection phenomena," Am. J. Phys. **35**, 177–186 (1967).

[2]L. I. Schiff, *Quantum Mechanics* (McGraw-Hill, New York, 1968), 3rd ed., pp. 104–109.

[3]E. Merzbacher, *Quantum Mechanics* (Wiley, New York, 1970), 2nd ed., pp. 110–114.

[4]D. S. Saxon, *Elementary Quantum Mechanics* (Holden-Day, San Francisco, 1968), pp. 155–166.

[5]A cutoff harmonic oscillator potential was used as an example in obtaining a numerical solution of the one-dimensional Schrödinger equation. C. K. Manka, "More on numerical solutions to simple one-dimensional Schrödinger equations," Am. J. Phys. **40**, 1539–1541 (1972).

[6]A three-dimensional truncated harmonic oscillator potential without a barrier was used in a discussion of nuclear shell structure. M.G. Mayer and J. H. D. Jensen, *Elementary Theory of Nuclear Shell Structure* (Wiley, New York, 1957), p. 52.

[7]Reference 3, pp. 54–56.

[8]The quantity $|1 - e^{2i\delta}|^2$ is called the "scattering coefficient." Reference 3, p. 114.

[9]Reference 3, pp. 86–87.

[10]Reference 3, pp. 47–48, 154–156.

The effects of coefficient of restitution variations on long fly balls

David T. Kagan
Physics Department, California State University, Chico, Chico, California 95929-0202

(Received 2 December 1988; accepted for publication 14 March 1989)

The coefficient of restitution of major league baseballs is required to be 0.546 ± 0.032. These allowed variations affect the launch velocity and ultimately the range of fly balls. The variations in the range for well-hit balls are calculated here to be on the order of 15 ft. These calculations provide an interesting collection of mechanics problems that might be of interest for undergraduate students.

I. INTRODUCTION

The coefficient of restitution for a collision is the ratio of the final relative velocity to the initial relative velocity of the colliding objects. The coefficient of restitution of a major league baseball is required to be 0.546 ± 0.032.[1,2] The question raised here is how will the allowed variations in the coefficient of restitution affect the distance traveled by a well-hit ball?

The first step toward the answer is to find the effect of coefficient of restitution variations on the velocity of the ball as it leaves the bat, referred to here as the launch velocity. Next, the range for a baseball as a function of the launch velocity must be studied. To keep some resemblance to reality, air resistance must be included. Finally, the two results can be put together to find the variations in the range due to fluctuations in the coefficient of restitution. Since the interest here is just the variations in the range, as opposed to the values of the range, and because it is often easier and frequently more accurate to calculate variations, as opposed to the actual values themselves, only the variations will be found.

II. THE VARIATION OF THE LAUNCH VELOCITY WITH THE COEFFICIENT OF RESTITUTION

The collision viewed from a coordinate system moving with the center of mass of the bat at the moment just before impact is shown in Fig. 1. According to the standard assumptions, the bat can be treated as a free body.[3] The equations needed to describe the ball–bat collision come from the conservation of linear momentum, the conservation of angular momentum, and the definition of the coefficient of restitution. These equations are

$$mv_0 = MV - mv, \tag{1}$$

$$I\omega_0 - mv_0 b = I\omega + mvb, \tag{2}$$

$$e = (v + V - \omega b)/(v_0 + \omega b), \tag{3}$$

where m is the mass of the ball, M is the mass of the bat, I is the moment of inertia of the bat about the center of mass, v_0 and v are the initial and final velocities of the ball, V is the final velocity of the center of mass of the bat, ω_0 and ω are the initial and final angular velocities of the bat, b is the